C-1027-Induced Alterations in Epstein−Barr Viral DNA Replication in Latently Infected Cultured Human Raji Cells: Relationship to DNA Damage†

Mary M. McHugh and Terry A. Beerman*

Department of Pharmacology and Therapeutics, Roswell Park Cancer Institute, Elm and Carlton Streets, Buffalo, New York 14263

Received February 9, 1999; Revised Manuscript Received March 29, 1999

ABSTRACT: This study is the first detailing drug-induced changes in EBV DNA replication intermediates (RIs). Both EBV replication inhibition and damage induction were studied in latently infected human Raji cells treated with the enediyne DNA strand-scission agent C-1027. Analysis of RIs on two-dimensional agarose gels revealed a rapid loss in the EBV bubble arc. When elongation of nascent chains was blocked by aphidicolin, this loss was inhibited, suggesting that C-1027-induced disappearance of RIs was related to maturation of preformed replication molecules in the absence of initiation of new RIs. C-1027 damage to EBV DNA was limited at concentrations where loss of the bubble arc was nearly complete, and none was detected within the replicating origin (ori P)-containing fragment, indicating that replication inhibition occurred in trans. By contrast, the non-nuclear mitochondrial genome was insensitive to replication inhibition but highly sensitive to damage induced by C-1027. C-1027-induced trans inhibition of nuclear but not mitochondrial DNA replication is consistent with a cell cycle checkpoint response to a DNA-damaging agent. EBV replication and Raji cell growth were inhibited at equivalent C-1027 doses.

DNA damage initiates a cascade of cellular events (*1*−*3*), which can lead to arrest in any phase of the cell cycle, including S-phase (*4*, *5*), in lower organisms as well as in mammalian cells (*1*, *6*). Replication can be inhibited in cis, that is by production of a lesion which physically blocks initiation or elongation of the replication fork. This type of inhibition might occur with high levels of a DNA-damaging agent or with specific types of DNA damage (e.g., alkylation (*4*), cisplatin adducts (*5*), etc.). Replication inhibition also may occur in trans, in which replication fork movement is blocked by alterations in or inhibition of essential replication factors (*6*−*8*). Cell cycle checkpoint regulation is a cellular response to DNA damage which is associated with trans inhibition of DNA replication (*6*, *9*, *10*).

In concert with cis or trans effects on DNA replication, damage can inhibit replication at the level of initiation or elongation (*11*−*13*). Earlier studies using sucrose gradient techniques suggested that irradiation and certain enediyne DNA strand-scission agents blocked replication primarily at the level of initiation (*14*, *15*). In contrast, alkylation with cisplatin inhibited both initiation and chain elongation at the site of the DNA lesion (*16*). More recently, two-dimensional (2-D) agarose gel electrophoresis (*17*) has been used to study changes in DNA replication intermediates. Examination of SV40 replication intermediates on 2-D gels indicated that elongation was blocked by agents that interfere with the incorporation of dNTPs into DNA (*17*, *18*), while initiation was inhibited by treatment with very low concentrations of either adozelesin, a DNA alkylator (*19*), or C-1027, an enediyne strand-scission agent (*20*).

While providing novel information about drug effects on replicating molecules, SV40 was not an ideal system for studying "normal" eucaryotic replication, since an infected host cell ceases to divide within one round of replication after viral infection in a process terminating in cell lysis and death (*21*). Thus, metabolic responses to drug-induced DNA damage could differ in SV40 lytically infected cells and in immortalized cells in culture. In addition, the SV40 replicon is very small (5243 bp) compared to the average-sized mammalian replicon (2.0×10^5 bp (*22*)).

The large-sized (1.84×10^5 bp (*23*)) EBV episome in human Raji cells (*22*) provides an excellent model of a mammalian replicon in which both damage induction and replication effects can be quantitated in immortalized cells in culture. Since the EBV genome is circular, the overall damage is readily quantitated by forms conversion analysis (*24*). Much of the EBV genome has been sequenced, allowing for detection of damage at specific sites (*25*). The locations of some replication origins have been defined, and initiation events are distributed over a broad region resembling initiation of replication in mammalian chromosomal loci. (*26*). Replication of the EBV genome occurs during S-phase (*27*) along with cellular genomic DNA and is dependent on the cellular replication machinery in the nucleus (*28*, *29*). Recently, the isolation of EBV replication intermediates has been described (*26*).

This study is the first assaying drug-induced changes in EBV replication intermediates. Raji cells were treated with

† This study was supported in part by grants from the National Cancer Institute (CA 77491 and CA 16056).

* To whom correspondence should be addressed. Tel: 716-845-3443. Fax: 716-845-8857. E-mail: beerman@sc3101.med.buffalo.edu.

10.1021/bi9903143 CCC: $18.00
Published on Web 05/07/1999

C-1027, an enediyne-chromophore containing DNA strand-scission anticancer agent (*30*, *31*) which inhibits initiation of SV40 replication in trans in lytically infected BSC-1 cells (*20*). Electrophoresis of EBV origin-containing fragments on 2-D agarose gels was used to distinguish C-1027 effects on replication initiation and elongation. EBV DNA damage was quantitated to assess whether replication was affected in cis or in trans. Drug levels inducing EBV replicative effects were assayed for cell growth inhibition. The amount of C-1027-induced damage to nuclear Raji cell genomic and non-nuclear (mitochondrial) DNA damage also was determined, and changes in mitochondrial replication intermediates were examined.

EXPERIMENTAL PROCEDURES

Chemicals. C-1027, a generous gift from Taiho Pharmaceuticals Co., Ltd, Saitama, Japan, was diluted in water and stored at −20 °C. [2-^{14}C]Thymidine (56 mCi/mmol) was from Moravek Biochemical (Brea, CA). [α-^{32}P]dCTP and Genescreen membranes were from Dupont NEN (Boston, MA). DECA-prime II DNA-labeling kit was from Ambion (Austin, TX). Agarose MP, used for pulsed-field gels, and proteinase K were from Boehringer Mannheim (Indianapolis, IN). High-strength analytical grade agarose used for 2-D gels was obtained from Bio-Rad Laboratories (Hercules, CA). Incert agarose was obtained from FMC Bioproducts (Rockland, ME) and prepared in phosphate-buffered saline (PBS). All other chemicals were of reagent grade.

Cell Culture. Conditions for maintenance of Raji cell cultures were described earlier (*24*). Briefly, cells were maintained in suspension at (0.5−3) × 10^6 cells/mL in RPMI 1640 medium supplemented with 10% Hyclone bovine calf serum.

C-1027 Treatment and Preparation of DNA. Logarithmically growing Raji cells (0.5 × 10^6/mL) were radiolabeled for 24 h with [2-^{14}C]thymidine (0.0125 μCi/mL) to permit detection of Raji cell genomic DNA. Labeled cells were adjusted to 1 × 10^6/mL and treated with C-1027. After the appropriate incubation time at 37 °C, cells were harvested by centrifugation and washed twice in PBS. Three cell dilutions in 0.66% agarose were prepared. For detection of EBV RIs, cells were adjusted to 2.6 × 10^8 cells/mL (cell stock A). Since mitochondrial RIs could be detected using 10-fold less DNA, cells were diluted to 2.6 × 10^7 cells/mL (cell stock B). For detection of the damage to the EBV episome, Raji cell genomic DNA, or mitochondrial DNA, cells were diluted to 1.43 × 10^7/mL (cell stock C). For detection of EBV or mitochondrial RIs, 0.039 mL of cell stock A (1 × 10^7 cells) or B (1 × 10^6 cells), respectively, was aliquoted into 2.2 mL graduated microfuge tubes (Laboratory Product Sales, Rochester, N. Y), and 0.013 mL of 1.0 mg/mL proteinase K in 1% sodium dodecyl sulfate, 100 mM EDTA, pH 8.0 (lysis A) was added. For detection of the damage to the EBV episome, Raji cell genomic DNA, or mitochondrial DNA, 0.021 mL of cell stock C (3 × 10^5 cells) was aliquoted, and 0.007 mL of 1% Sarcosyl, 0.5 M EDTA, pH 8.0, 2 mg/mL proteinase K (lysis B) was added. In all cases, samples were mixed only once (finger-tapped, three times) after the addition of lysis buffer. Samples were incubated for 2 h at either 37 °C (EBV and mitochondrial RI samples) or 55 °C (EBV, genomic, and mitochondrial DNA damage detection). After incubation, samples were spun in a microfuge for 2 s and placed at 4 °C for 0.5 h to allow a hardened agarose plug to form. TE (0.5 mL) was added to each tube, samples were tapped to suspend the plug, and plugs were stored at 4 °C for ≥16 h to allow for diffusion of detergent, proteinase K, and other impurities from the plug. The plugs, which could be stored for several months without DNA degradation, were used for pulsed-field gel and agarose gel analysis of nuclear and mitochondrial DNA damage, respectively, and for 2-D gel electrophoresis of EBV and mitochondrial RIs, as described below.

Analysis of EBV and Mitochondrial RIs by 2-D Gel Electrophoresis. Isolated DNA embedded in agarose plugs as described above was prepared for 2-D gel electrophoresis by restriction enzyme digestion. The day of restriction, each plug was washed by placing it in a 10-fold excess of restriction enzyme buffer (0.5 mL) for 0.5 h at 4 °C. The wash was repeated twice. The plug was drained and heated at 68 °C for 10 min to melt the agarose, then placed at 37 °C. A 0.028 mL aliquot of restriction enzyme mix (35 units of each enzyme in 1× restriction buffer) was added directly into the viscous 0.052 mL of DNA, and samples were finger-mixed. Samples were finger-mixed every 15 min for 2 h, and then every 0.5 h for a total of 4 h of incubation. The restricted DNA was loaded into the wells of 0.6% agarose gels, then placed at 4 °C for 0.5 h to harden the agarose in the well before submerging the gel in electrophoresis buffer. After electrophoresis at 0.84 V/cm for 20 h in 1× TAE, 0.1 μg/mL ethidium bromide, lanes were visualized over an ultraviolet light source and cut out and placed in a slot cut in the top of a 1% agarose gel. The second dimension gel was electrophoresed at 4 V/cm for 20 h in 0.5× TBE, 0.5 μg/mL ethidium bromide.

Southern Blots and DNA Hybridization. All gels were Southern blotted to Genescreen, and DNA was UV cross-linked to the blots according to the manufacturer's instructions. Blots were hybridized to the appropriate DNA probe which had been radiolabeled with [α-^{32}P]dCTP using the DECAprime II DNA-labeling kit. After hybridization, the [^{32}P]-radiolabeled DNA was detected by phosphorimaging. Images were analyzed using ImageQuant software (Molecular Dynamics, Sunnyvale, CA). To detect EBV DNA, blots of 2-D gels were hybridized to the [^{32}P]-radiolabeled 5.9 kb *Bam*HI-*Eco*RI restriction enzyme digestion fragment of the EBV episome from B95-8 cells containing ori P, the latent origin of EBV replication (*32*). To detect mitochondrial DNA, blots of 2-D gels were hybridized to the [^{32}P]-radiolabeled human mitochondrial DNA probe (41−2578 bp on the human mitochondrial DNA map (*33*)) generously provided by Dr. A. Chomyn in the laboratory of Dr. G. Attardi, California Institute of Technology, Pasadena, California.

Quantitation of EBV RIs. The effects of C-1027 on EBV RIs (see Figure 1) were determined from phosphorimages of Southern blots as described earlier for SV40 DNA RIs (*20*). Briefly, identical ellipses were inserted over the tips of the fork arc (FA) and the bubble arc (BA) (i.e., to include the most intense signal), the 1n spot (1n), and over a portion of the phosphorimage in which no DNA was located (to provide a background value [BG]). The volumes of the ellipses were quantitated, and the fork arc signal was

FIGURE 1: Pattern of EBV DNA RIs after electrophoresis on 2-D agarose gels. Raji cell DNA was restriction enzyme digested with *Pvu*II and *Bam*HI, and replication intermediates were visualized by hybridization to a [^{32}P]-radiolabeled EBV ori P-containing fragment. Electrophoresis conditions, Southern blotting, and hybridization methods are described in Experimental Procedures.

calculated according to the following formula:

$$\text{FA signal} = \frac{(\text{FA} - \text{BG})}{(1\text{n} - \text{BG})/(1\text{n}_{\text{control}} - \text{BG})}$$

where 1n and $1n_{control}$ refer to the amount of unreplicated *Pvu*II-*Bam*HI restricted EBV DNA in the sample and in the control, respectively. Changes in the bubble arc (BA) were calculated by substituting the values obtained for the BA for FA in the above formula.

C-1027-Induced Double-Strand Damage to Nuclear (i.e., EBV and Cellular Genomic) and Non-nuclear (Mitochondrial) DNAs. Damage to genomic DNA and to the EBV episome was detected using the pulsed-field gel electrophoresis conditions described earlier (*24*). Briefly, plugs containing 3×10^5 cells were loaded into the wells of a 0.75% agarose gel (Agarose MP), and 0.5% molten Incert agarose was added to seal each well. To provide a positive measure of double-strand DNA damage, at least four DNA samples isolated from Raji cells X-irradiated with 200−12000 rads were loaded on each pulsed-field gel in addition to drug-treated samples. Gels were electrophoresed in 0.5× TBE buffer for 18 h at 200 V with ramped pulse conditions of 0.1−100 s using a BioRad Chef DR II and subjected to Southern blotting as described above. For detection of damage to total cellular DNA, [^{14}C]-radiolabeled DNA was detected on the Southern blots by phosphorimaging prior to hybridization to [^{32}P]-radiolabeled probe. Image analysis and quantitation of double-strand break (DSB) induction in cellular genomic DNA was performed as described earlier (*13*). Damage to total cellular DNA was converted to rad equivalents by comparing the loss of [^{14}C]-radiolabeled DNA from the well in C-1027-treated samples with that observed in DNA from cells irradiated with 200−12000 rads. After [^{14}C] detection, the same blots were hybridized to the [^{32}P]-radiolabeled EBV DNA probe described above. After hybridization, blots were covered with plastic wrap to block the [^{14}C] signal and the [^{32}P]-radiolabeled EBV detected by phophorimaging. An increase in EBV Form III was indicative of DSB damage to the EBV episome. C-1027-induced DSB damage to the EBV episome was converted to rad equivalents by comparing the increase in Form III in DNA from C-1027-treated cells with that in cells subjected to 200−12000 rads. X-irradiation induces a known level of double-strand damage. Rad equivalents were converted to double-strand breaks per nucleotide by multiplying the rad equivalent damage by (8.3×10^{-14} DSB Da^{-1} rad^{-1}) × (320 Da) (*13*).

Damage to mitochondrial DNA was detected by the separation of topological forms on agarose gels (*34*). Plugs containing 3×10^5 cells were drained and placed at 68 °C for 10 min to melt the agarose. Samples were loaded into the wells of a 0.8% agarose gel, and the gel was placed at 4 °C for 0.5 h to harden the agarose in the wells. Mitochondrial forms were separated by electrophoresis at 6 V/cm for 18 h in 1× TBE. After electrophoresis, gels were Southern blotted and hybridized to the [^{32}P]-radiolabeled mitochondrial probe described above. The blots were covered with plastic wrap, and the [^{32}P]-mitochondrial signal was detected by phosphorimaging. Increases in mitochondrial Form III DNA were indicative of DSB damage to mitochondrial DNA. DSB in mitochondrial DNA were quantitated as described earlier for SV40 DNA (*13*). Briefly, the fractional increase in mitochondrial Form III was divided by the number of mitochondrial nucleotides (2×16500) to give the number of DSBs per nucleotide.

Cell Growth Inhibition. Logarithmically growing cells were adjusted to 0.5×10^6/mL in 1640 medium and treated with 0.1−100 pM C-1027. Cells were counted 3 days after C-1027 addition.

RESULTS

This study examined the effect of C-1027 on EBV DNA replication in immortalized cultured human Raji cells latently infected with the EBV virus. Since in Raji cells the amounts of EBV DNA and its replication intermediates are limited (*26*), an isolation method was used which optimized DNA recovery (*35*). After intact cells were mixed with molten agarose, proteins were digested by incubation with proteinase K. The agarose then was hardened at 4 °C, and impurities were removed by suspending the hardened agarose plug at 4 °C in TE buffer overnight. DNA isolated by this method was used for electrophoresis of EBV RIs on 2-D gels and for analysis of EBV and genomic DNA damage on pulse-field gels.

2-D Agarose Gel Analysis of EBV Replication Intermediates. Samples were restriction digested with *Pvu*II and *Bam*HI. *Pvu*II cuts EBV at sites 6776 and 12412, producing a fragment that encompasses ori P (7315−9312 bp on the EBV map) (*36*). *Bam*HI restriction was necessary to reduce the signal from repetitive sequences outside the ori P fragment which hybridized to the [^{32}P]-radiolabeled EBV probe. Restricted DNA was electrophoresed on neutral 2-D agarose gels. 2-D agarose gel electrophoresis separates replication intermediates on the basis of size in the first dimension and size and shape in the second dimension (*20*). The migration pattern of EBV replicating intermediates after electrophoresis of the 5637 bp ori P fragment on a second dimension agarose gel is shown in Figure 1 and is described below. In Raji cells, EBV replication is bidirectional and can initiate over a range of sequences within and outside ori P (*26*). The bubble arc consists of replicating molecules (bubbles) which have initiated at or near ori P but have not yet elongated beyond the restriction sites bordering the ori P-containing fragment. The fork arc consists of "Y"-shaped molecules which have replicated to differing extents. As shown elsewhere (*26*), the EBV fork arc signal is more intense than the bubble arc signal. When replicating molecules were quantitated as described in Experimental Procedures, the fork arc represented 0.92 (±0.018 SEM) of the total RIs (i.e., fork plus bubble arcs). While forks may be

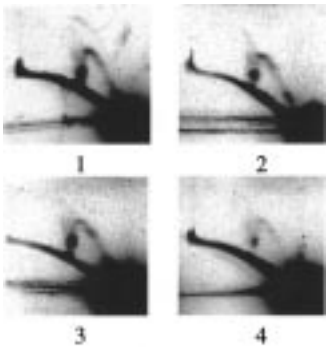

FIGURE 2: C-1027 effects on EBV DNA replication intermediates. Cells were treated for 0.5 h with (1) 0, (2) 0.1 nM, or (3) 10 nM C-1027, or for 2 h with (4) 10 nM C-1027. To detect EBV RIs, samples were assayed as described in Figure 1. Each panel shows Southern blots of DNA from 7×10^6 cells.

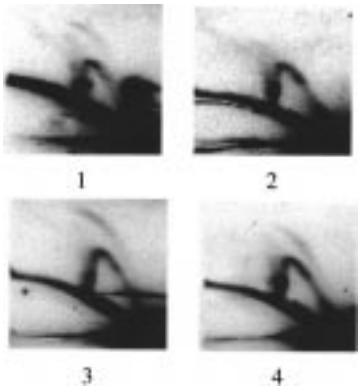

FIGURE 3: Aphidicolin inhibition of C-1027 effect on EBV RIs. Treatment of cells for 5 min with 5 μM aphidicolin was followed by addition of C-1027 and incubation in the presence of both agents for 0.5 h. Representative Southern blot of DNA from cells treated with (1) no drug, (2) 10 nM C-1027, (3) 5 μM aphidicolin, or (4) 10 nM C-1027 plus 5 μM aphidicolin. Samples were assayed as described in Figure 1.

produced by damage to replicating bubbles, the large number of forks observed likely results from progressive replication of DNA already initiated at multiple sites outside the ori P fragment (*26*). The sum of both bubble and fork arcs is minimal compared to the 1n spot (the fraction of nonreplicating ori-P fragments) and equals only 0.002 (±0.0002 SEM) of the total EBV signal, indicating that only a small proportion of the isolated EBV DNA consists of replicating genomes. Random termination (i.e., over a range of sequences) is indicated on the figure by a broad area of radioactivity between the left tip of the fork and bubble arc. Although bidirectional, replication is asynchronous, due to forks pausing at discrete sites (e.g., at the Eber 1 and Eber 2 genes (*26*)). The accumulation of replicating molecules at pause sites results in an especially strong DNA signal as seen in Figure 1. The arc of linear molecules consists of cellular genomic DNA. The intense signal associated with this arc indicates homology between portions of genomic DNA and the EBV ori-P probe.

C-1027 Effects on EBV RIs. The effect of C-1027 on EBV replication intermediates is shown in Figure 2. Compared to the control (panel 1), 0.5 h treatment with 0.1 nM C-1027 (panel 2) caused a near total loss of the bubble arc signal with little or no effect on the fork arc or on molecules with terminating structures. The intensities of the fork arc and of terminating molecules decreased after 0.5 and 2 h of incubation with 10 nM C-1027 (panels 3 and 4). When quantitated as described in Experimental Procedures, a 2 h treatment with 10 nM C-1027 reduced the fork arc to 0.16 (±0.04 SEM) times the control value.

C-1027 Effects on Initiation. If C-1027 inhibits initiation but not elongation, formation of replicating bubbles should be blocked, while replicons already initiated should continue to elongate. As the replicating molecules elongate past the restriction sites, they will migrate as forks rather than as bubbles on a 2-D gel. Thus, reduced initiation in the absence of an elongation block would effect a decrease in the bubble arc. Mammalian genomic DNA replicates at a rate of 1.7−1.9 kb/min (*37*), and complete elongation of the 5637 bp ori p fragment should occur very rapidly (i.e., within 6−7 min[1]). Thus, in the absence of new initiation events, the ori P bubble arc should disappear rapidly. The rapid disappearance within 0.5 h of the bubble arc (see Figure 2) indicated that C-1027 inhibited initiation of EBV replication. In addition, C-1027 caused a much slower decrease over 2 h in the intensity of the fork arc. While the persistence of the fork arc could reflect an inhibitory effect on elongation, the eventual disappearance of the forks indicated that any elongation block was not complete.

Evidence that C-1027 inhibited initiation of EBV replication also was obtained by treating cells with C-1027 in the presence of the elongation inhibitor, aphidicolin (*20*). C-1027 inhibition of new initiation events would lead over time to the disappearance of EBV replication bubbles due to the elongation of replication forks past the restriction sites. By inhibiting elongation, aphidicolin should block the loss of replication bubbles, and the same proportion of EBV bubbles and forks should be observed in cells treated with both aphidicolin and C-1027 and those treated with aphidicolin alone.

The effect of aphidicolin on C-1027-induced changes in EBV RIs is shown in Figure 3. Compared to the control (panel 1), the bubble arc was reduced nearly completely by 10 nM C-1027 (panel 2), while no decrease was observed in the presence of aphidicolin alone (panel 3) after a 0.5 h treatment. The treatment of cells for 5 min with 5 μM aphidicolin prior to the addition of C-1027, followed by incubation in the presence of both agents for 0.5 h, prevented any C-1027-induced loss of the bubble arc (panel 4). These data suggested that the disappearance of the EBV bubble arc after C-1027 treatment resulted from elongation of preformed replication structures.

DNA Damage. C-1027 concentrations which inhibited EBV replication were assayed for DNA damage induction. Damage to the EBV episome was quantitated by topological forms analysis. EBV forms were separated by pulsed-field gel electrophoresis and detected by hybridization of Southern blots of pulsed field gels to the [^{32}P]-radiolabeled *Eco*RI-*Bam*HI EBV fragment described in Experimental Procedures. Figure 4A is a phosphorimage of the [^{32}P]-radiolabeled blot of a representative pulsed-field gel. A large amount of EBV signal was detected in the well at the top of the gel. This signal is contributed by DNA species which cannot readily enter the gel, such as relaxed circular form II (*24*, *38*), and EBV sequences which have integrated into genomic DNA

[1] Pausing could slow the replication rate somewhat.

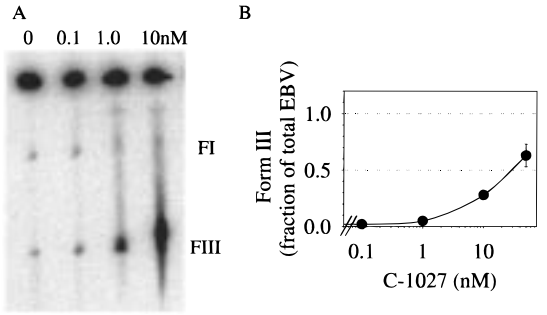

FIGURE 4: C-1027 damage to Raji cell EBV DNA. DNA was electrophoresed on a pulsed-field gel and analyzed on a Southern blot as described in Experimental Procedures. (A) Southern blot of a representative pulsed-field gel showing EBV DNA from cells treated for 0.5 h with 0, 0.1, 1.0, or 10 nM C-1027. FI is intact supercoiled Form I DNA, and FIII is linear Form III DNA (i.e., containing at least one double-strand break per molecule). (B) Graphic representation of the ratio of Form III EBV DNA to total EBV DNA with increasing C-1027 concentrations. Data are from five experiments and are expressed ±SEM.

(*39*). The amount of EBV Form III, indicative of double-strand damage, increased after 0.5 h with >0.1 nM C-1027. Figure 4B is a graphical representation of the increase in Form III expressed as a fraction of total EBV detected on the blot. No increase in Form III was observed with 0.1 nM C-1027, while a minimal increase was observed with 1.0 nM C-1027. Only with a very high C-1027 concentration (50 nM) was DSB damage observed in more than 50% of the EBV DNA as evidenced by >50% of the EBV signal migrating as Form III. Since the EBV bubble arc was reduced nearly completely with only 0.1 nM C-1027 (see Figure 2), much lower C-1027 concentrations were required for EBV replication inhibition than for detection of DSB damage to the EBV episome.

While damage to the entire EBV genome was very limited, replication inhibition could be directly inhibited if lesions were localized to the origin-containing fragment. Specific damage to the EBV ori P-containing fragment was assayed by sub-band formation as described earlier for SV40 DNA (*13*). Briefly, DNA isolated from Raji cells treated with 0−50 nM C-1027 was digested with *Eco*RI, *Pvu*II, and *Bam*HI to produce a 5097 bp ori P-containing fragment (i.e., 7315−12412 on the Raji cell EBV map (*23*)). This DNA was electrophoresed on a 0.6% agarose gel (1× TAE) for 17 h at 0.45 V/cm and Southern blotted. After hybridization to the [^{32}P]-radiolabeled *Kpn*I-*Eco*RI ori P fragment of B-95-8 EBV DNA[2] and phosphorimaging, only a single band was evident on the blot, both in the absence and in the presence of 1.0−50 nM C-1027 (see Figure 5). The absence of DNA sub-bands smaller than 5097 indicated that C-1027 did not induce DSB damage within the ori P-containing fragment.

Replication inhibition in the presence of very limited DNA damage reportedly is mediated by a trans acting mechanism (*40*) by which damage anywhere in the cellular genome can signal a halt in replication even at sites remote from the DNA lesion. Since 0.1 nM C-1027 strongly inhibited EBV replication while inducing very limited damage to the EBV genome

[2] The *Kpn*I-*Eco*RI fragment (7315−10312 bp on the EBV map) hybridizes to the ori P origin-containing fragment. The *Eco*RI−*Bam*HI probe described in the earlier figures contains a portion of the *Bam*HI repetitive sequence and can hybridize to other regions of the genome outside the origin fragment.

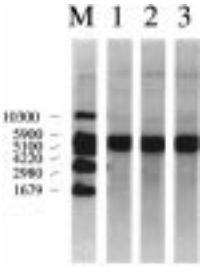

FIGURE 5: Absence of C-1027-induced damage within the EBV ori P fragment. Raji cell DNA was isolated from cells treated with 0−50 nM C-1027, digested with *Eco*RI, *Pvu*II, and *Bam*HI, and electrophoresed on a 0.6% agarose gel (1× TAE) for 17 h at 0.45 V/cm. The gel was Southern blotted and hybridized to the [^{32}P]-radiolabeled *Kpn*I-*Eco*RI[2] ori P-containing fragment of B-95-8 EBV DNA. The phosphorimage shows the 5097 bp ori P fragment from cells treated with the following: lane 1, 0; lane 2, 1.0 nM; and lane 3, 50 nM C-1027. Lane M shows the migration of EBV size markers from 1679 to 10300 bp long.

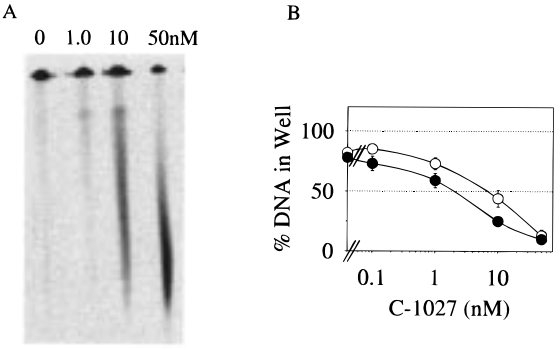

FIGURE 6: C-1027 damage to Raji cell genomic DNA. DNA was electrophoresed on a pulsed-field gel and analyzed on a Southern blot as described in Experimental Procedures. (A) Southern blot of a representative pulsed-field gel showing [^{14}C]-radiolabeled genomic DNA from cells treated for 0.5 h with 0, 1.0, 10, or 50 nM C-1027. (B) Graphic representation of DNA remaining in the well after electrophoresis of [^{14}C]-radiolabeled DNA from cells treated with C-1027 for 0.5 h (●) or 2 h (○). Radioactivity per lane was summed, and the amount remaining in the well was expressed as a percent of the total radioactivity. Data are from five experiments and are expressed ±SEM.

(see Figures 2 and 4), the extent of damage to nuclear genomic DNA also was determined. Figure 6A shows the migration on a pulsed-field gel of [^{14}C]-radiolabeled genomic DNA from Raji cells treated for 0.5 h with 0−50 nM C-1027. A decrease in the amount of [^{14}C]-DNA remaining in the well, indicative of DNA damage, was detectable with >1.0 nM C-1027. Figure 6B is a graphic representation of the decrease in DNA in the well occurring 0.5 and 2 h after C-1027 addition. In control samples (no C-1027), 0.8 of the DNA remained in the well. After treatment for 0.5 or 2 h with 1.0 nM C-1027, the amount of DNA in the well was reduced to 0.59 (±0.055 SEM) and 0.73 (±0.047 SEM) of the total DNA, respectively (or 750 and 460 DSB/cell, respectively, when calculated as described earlier (*13*)). That damage at 0.5 h was slightly higher than at 2 h suggested limited repair of genomic DNA at later times after C-1027 addition. EBV replication was strongly inhibited after treatment for 0.5 h with 0.1 nM C-1027 (see Figure 2). At this dose, the PFG method was not sensitive enough to detect DSB damage to cellular genomic DNA. However, if damage induction is assumed to be linear, extrapolation of the damage induced with 1.0 nM predicted that 0.1 nM C-1027 induced

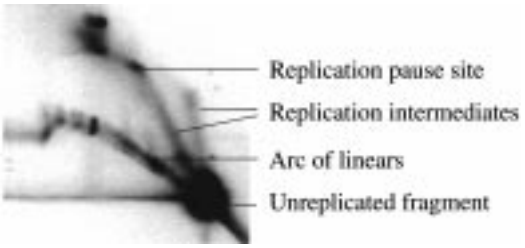

FIGURE 7: Pattern of mitochondrial DNA RIs after electrophoresis on 2-D agarose gels. Raji cell DNA was restriction enzyme digested with *Eco*RV. Electrophoresis conditions, Southern blotting, and hybridization to a [^{32}P]-radiolabeled mitochondrial probe are described in Experimental Procedures.

75 DSB/cell in genomic DNA. Thus, DSB damage was induced in cellular genomic DNA at C-1027 doses which inhibited EBV replication.

2-D Agarose Gel Analysis of Mitochondrial RIs. The above data suggested that C-1027 strongly inhibited nuclear EBV replication in trans. If replication inhibition resulted from a cell cycle checkpoint response, replication of a non-nuclear DNA target might not be similarly affected. The effect of C-1027 on the replication of non-nuclear DNA was examined by assaying C-1027 effects on mitochondrial RIs and induction of mitochondrial DNA damage. RIs associated with the heavy-strand origin of mitochondrial replication (ori H) were prepared by *Eco*RV restriction enzyme digestion of Raji cell DNA. This enzyme cuts human mitochondrial DNA at sites 13754 and 3181, producing a fragment encompassing ori H (i.e., 16000−200 on the human mitochondrial DNA map (*41*)). Restricted DNA was electrophoresed on 2-D agarose gels, and mitochondrial RIs were detected by Southern blot hybridization as described in Experimental Procedures. Figure 7 is a phosphorimage of a Southern blot of a representative gel showing the 2-D migration pattern of the Raji cell mitochondrial *Eco*RV ori H-containing fragment[3]. Molecules which migrated in a nonlinear fashion were identified as replication intermediates. The intense spots of radioactivity at discrete sites along RI arcs suggest the location of replication pause sites (*42*, *43*). The positions of the unreplicated fragment (1n spot) and the arc of linears also are indicated.

C-1027 Effects on Mitochondrial RIs. The effect of C-1027 on mitochondrial RIs is shown in Figure 8. Mitochondrial RIs were much more resistant than EBV RIs to C-1027 treatment. After 0.5 h of incubation with 1.0 and 50 nM C-1027 (panels 2 and 3) or 2 h with 50 nM C-1027 (panel 4), mitochondrial RIs were similar to those in the control (panel 1). Some pause sites showed increased intensity after a 2 h treatment with 50 nM C-1027, suggesting that higher C-1027 concentrations induce a decrease in the rate of mitochondrial replication (*44*).

C-1027-Induced Mitochondrial DNA Damage. Damage to the non-nuclear mitochondrial DNA target was assayed by agarose gel migration of mitochondrial DNA topological forms as described elsewhere (*34*) and in Experimental Procedures. Mitochondrial sequences were detected on Southern blots by hybridization to the [^{32}P]-radiolabeled

[3] Since mitochondrial replication is unidirectional, the 2-D gel migration pattern of the ori H-containing fragment differs from that observed with the ori P-containing fragment of EBV which replicates bidirectionally.

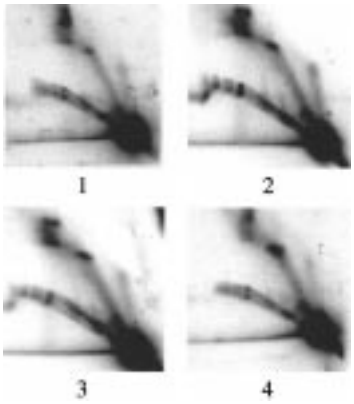

FIGURE 8: C-1027 effects on Raji cell mitochondrial DNA replication intermediates. Cells were treated for 0.5 h with (1) 0, (2) 1.0, or (3) 50 nM C-1027, or for 2 h with (4) 50 nM C-1027. To detect mitochondrial RIs, samples were assayed as described in Figure 7. Each panel shows Southern blots of DNA from 1 × 10^6 cells.

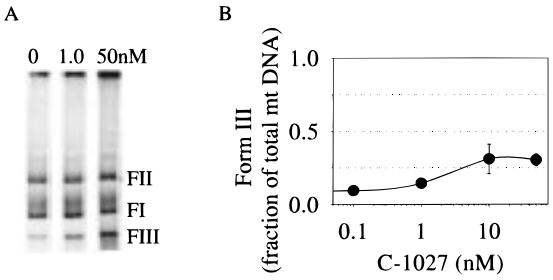

FIGURE 9: C-1027 damage to Raji cell mitochondrial (mt) DNA. DNA was electrophoresed on a 0.8% agarose gel and detected on a Southern blot as described in Experimental Procedures. (A) Phosphorimage of a representative Southern blot of mitochondrial DNA from cells treated with 0, 1.0, or 50 nM C-1027. FI and FIII topological forms are described in Figure 4. FII is relaxed circular Form II DNA with at least one single-strand break per molecule. (B) Graphic representation of the ratio of Form III mitochondrial DNA to total mitochondrial DNA with increasing C-1027 concentrations. Data are from five experiments and are expressed ±SEM.

human mitochondrial DNA probe described in Experimental Procedures. Figure 9 shows C-1027 damage to mitochondrial DNA. Panel A is the phosphorimage of a Southern blot of a representative gel showing electrophoretic migration of Raji cell mitochondrial DNA forms. Increases in mitochondrial Form III, indicative of double-strand damage, were noted after a 0.5 h treatment with ≥1.0 nM C-1027. In Panel B, this increase in Form III is plotted graphically. Form III increased to 30% (±4 SEM) of the total mitochondrial DNA with 10 and 50 nM C-1027. While DSB damage increased significantly with >1.0 nM C-1027, effects on mitochondrial RIs were limited even with 50 nM C-1027 (see Figure 8, panels 3 and 4). Thus, higher C-1027 concentrations were required for the detection of mitochondrial replication inhibition than for DSB damage to the mitochondrial genome. Since only C-1027 concentrations associated with high levels of damage induction produced an effect on mitochondrial RIs (i.e., an increase in pause site intensity), inhibition of mitochondrial replication probably occurs in cis.

Comparison of C-1027-Induced Double-Strand Damage to Nuclear (i.e., EBV and Cellular Genomic) and Non-nuclear (Mitochondrial) DNA. Since EBV and mitochondrial DNA differed in their replication response to C-1027, the

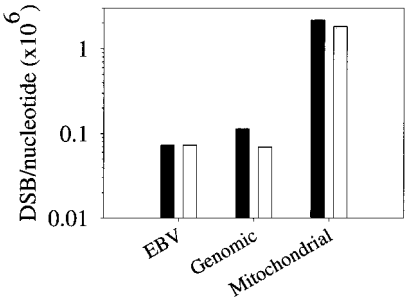

FIGURE 10: Summary of C-1027-induced damage to Raji cell nuclear (EBV and cellular genomic) and non-nuclear (mitochondrial) DNA. Cells were incubated with 1.0 nM C-1027 for 0.5 h (■) or 2 h (□). DNA damage was quantitated as described in Experimental Procedures and expressed as double-strand breaks (DSB) per nucleotide. Data are the average of four experiments.

levels of damage induced in nuclear (EBV and cellular genomic) and mitochondrial DNA were compared. Low C-1027 levels (1 and 10 nM) induced similar increases in Form III in EBV and mitochondrial DNA (see Figures 4 and 9, respectively). Form III results from at least one double-strand break per intact circular molecule (i.e., 1/184113 bp or 1/16500 bp for EBV or mitochondrial DNA, respectively). Thus, C-1027 apparently directed greater numbers of lesions per base pair to mitochondrial than to EBV DNA. To directly compare the C-1027 damage induced in nuclear (i.e., EBV and cellular genomic) and in non-nuclear (mitochondrial) DNA, the number of double-strand breaks induced per nucleotide (NT) was quantitated as described in Experimental Procedures. Figure 10 shows damage to EBV, cellular genomic, and mitochondrial DNA after 0.5 and 2 h of treatment with 1.0 nM C-1027. After 0.5 h, slightly less damage (1.5-fold) was observed in EBV DNA (0.073 DSB/10^6 NT) than in cellular genomic DNA (0.114 DSB/10^6 NT). Damage induced in mitochondrial DNA (2.165 DSB/10^6 NT) was 30 and 19 times that in EBV and cellular genomic DNA, respectively. After 2 h, the level of damage to cellular genomic DNA had decreased to that of EBV DNA, suggesting that some repair to genomic DNA had occurred. No change in EBV damage, and hence no apparent repair of EBV DNA, was observed after 2 h. While a slight decrease in mitochondrial DNA damage (to 1.82 DSB/10^6 NT) was observed after 2 h, the damage to mitochondrial DNA remained at least twenty-five times that induced in nuclear DNA (either EBV or cellular genomic). Even when the damage was expressed per genome, 0.5 h of incubation with 1.0 nM C-1027 induced a DSB in 1/14 mitochondrial genomes and in 1/37 EBV genomes. Thus C-1027 induced higher amounts of damage in mitochondrial compared to nuclear DNA.

Cell Growth Inhibition Whether decreases in EBV replication were indicative of overall Raji cell growth inhibition was examined. Figure 11 shows the decrease in Raji cell growth assayed as described in Experimental Procedures 3 days after treatment with 0.1−100 pM C-1027. A 50% decrease in cell growth was observed with 27 pM C-1027 (i.e., 0.057 pmol C-1027/10^6 cells). Nearly complete loss of the EBV bubble arc was observed with 0.1 nM C-1027 (i.e., 0.1 pmol C-1027/10^6 cells) (see Figure 2). Thus, similar C-1027 concentrations affected changes in EBV replication and Raji cell growth.

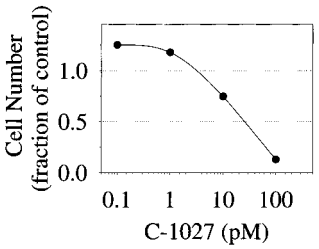

FIGURE 11: Cell growth inhibition by C-1027. The assay for cell growth inhibition was described in Experimental Procedures. Cells were counted 3 days after the addition of C-1027.

DISCUSSION

The structure of replication intermediates has been a focus of recent reports on mammalian DNA replication (*44*−*47*). Recently, other workers described the 2-D gel electrophoretic pattern of EBV replication intermediates from latently infected human Raji cells (*26*). The present report describes DNA strand-scission drug-induced alterations in EBV replication intermediates and their relationship to DNA damage.

Examination of the pattern of replication intermediates on 2-D gels revealed a rapid decrease in EBV replication bubbles when Raji cells were treated with low nanomolar concentrations of C-1027. The EBV bubble arc disappeared within 0.5 h, while the fork arc intensity decreased more slowly and still was visible 2 h after C-1027 treatment. These observations, coupled with the ability of the elongation inhibitor aphidicolin to prevent bubble arc disappearance, suggested that C-1027 inhibited initiation of new EBV replicons. If C-1027 inhibited initiation and not elongation, no new replication bubbles would be initiated while already initiated bubbles would continue to elongate. That C-1027 caused a more rapid decrease in the EBV bubble arc than in the fork arc probably is related to the large size of the EBV replicon (184 113 bp) and the time necessary for maturation of RIs. Replication forks would remain visible until the EBV molecules had completely replicated. Since the fork arc was reduced but still visible 2 h after treatment, up to 2 h may be required to complete a round of EBV replication.

DNA damage can inhibit replication in cis (i.e., by a direct effect on the DNA template) or in trans, by inducing a cell cycle checkpoint response which alters the levels of or interactions with key replication components. When the entire EBV genome was examined by pulsed-field gel electrophoresis, C-1027-induced double-strand lesions were few, but detectable. Approximately 1/370 EBV molecules[4] was damaged by 0.1 nM C-1027 treatment which effected nearly complete disappearance of the bubble arc. Since the fraction of replicating molecules also was limited, it was possible, though unlikely, that these lesions were localized to replicating molecules. However, when the ori P-containing fragment of EBV was isolated from Raji cells treated with 0.1−10 nM C-1027 and examined by electrophoresis on agarose gels (see Figure 5), no DSB damage (i.e., no fragments smaller than the ori P-containing fragment) was detected.

[4] EBV DNA DSB damage induced by treating Raji cells with 0.1 nM C-1027 was too low to quantitate using pulsed-field gel electrophoresis. This number (1/370 genomes) assumes that damage is linear and that 0.1 nM C-1027 will induce one-tenth of the number of DSB observed with 1.0 nM (i.e., 1/37 EBV genomes).

In addition to DSB, C-1027 also induces single-strand breaks (SSB) in intracellular DNA (*13*) which might inhibit the progression of replicating DNA in cis. SSBs were not detectable with the nondenaturing gel conditions described above. However, an earlier study with intracellular SV40 DNA showed that with 0.7−33 nM C-1027, the average SSB/DSB ratio was 2.0 (range = 2.9−1.4) (*13*). If 0.1 nM C-1027 induced 1.0 DSB/370 EBV molecules,[4] then no more than 1.0 SSB/127 EBV molecules would be expected. Thus, the inhibition of EBV replication initiation observed with as little as 0.1 nM C-1027 probably does not occur in cis.

Very limited DNA strand damage anywhere in the cellular genomic DNA can inhibit nuclear DNA replication and progression of cells through the cell cycle in trans (*1*−*3*). Radiation is an example of a trans acting DNA-damaging agent, which reportedly inhibits initiation of mammalian nuclear DNA replication and induces an S-phase cell cycle checkpoint response (*46*). Trans inhibition of initiation of SV40 DNA replication by C-1027 was reported earlier (*20*). That initiation of EBV replication was inhibited with C-1027 concentrations which induced low levels of DSB damage to cellular genomic and EBV DNA and no DSB damage in the ori P-containing fragment suggested that EBV replication also was inhibited in trans.

Whether C-1027-induced EBV DNA initiation inhibition is associated with a cell cycle checkpoint response is uncertain. Other workers have described C-1027-induced inhibition of S phase progression and cell cycle arrest in G2+M in hepatoma cells (*48*). Preliminary results using flow cytometry indicate that cytotoxic doses of C-1027 also induce Raji cell cycle arrest in G2+M (unpublished observation). Agents which slow S phase progression may alter the availability of replication initiation proteins such as cyclin A, cdk2, RPA-34 and RPA-70 (*49*), while a G2+M block has been associated with inhibition of topoisomerase II and chromatid decatenation (*50*).

C-1027 was much more inhibitory to EBV than to mitochondrial DNA replication. Other workers have shown that ionizing radiation also is inhibitory to nuclear DNA, but not mitochondrial DNA replication in human cells (*51*). That nuclear DNA replication is dependent on the cell cycle and occurs during S-phase (*52*) while mitochondrial DNA replication can occur throughout the cell cycle (*53*) may account for these differing effects. For example, agents which inhibit cell cycle progression should inhibit nuclear to a greater extent than non-nuclear (mitochondrial) DNA replication, resulting in an increased accumulation of mitochondrial mass per cell. Other workers have reported increased accumulation of mitochondria in cultured human cells after treatment with cytotoxic doses of either herbimycin A, a tyrosine kinase inhibitor (*54*), or fialuridine, a nucleoside analogue (*55*). An increase in mitochondrial DNA relative to total cellular genomic DNA also was observed after Raji cells were treated with a cytotoxic dose of C-1027 (unpublished observation). Both mitochondrial proliferation (*54*, *56*) and the accumulation of mitochondrial DNA (*57*) have been correlated with the induction of apoptosis which may result from an increased mitochondrial production of reactive oxygen species (*58*).

Preferential C-1027 strand break induction in mitochondrial compared to genomic DNA was described earlier in murine 935 cells (*34*). In the present study, greater amounts of C-1027-induced damage were observed in mitochondrial than in either EBV or cellular genomic DNA. Larger numbers of C-1027 lesions may inhibit mitochondrial replication in cis. For example, 2 h with 50 nM C-1027, which induced double-strand damage to 15% of the mitochondrial genomes (data not shown), also affected a change in intensity of the replication pause sites (see Figure 8, panel 4). Damage within a specific mitochondrial DNA molecule may halt replication of that molecule until the lesion has been removed. Thus, direct damage to mitochondrial genomes could promote a decrease in mitochondrial DNA replication.

The EBV episome is a good representative of a mammalian replicon and a facile model for investigating the relationship between drug-induced DNA damage, nuclear DNA replication and cell growth inhibition. The extent of damage induced in the EBV episome was equivalent to that in cellular genomic DNA, and concentrations of C-1027 which induced early EBV replication inhibition also inhibited Raji cell growth. No damage was observed in the EBV ori P region, making it unlikely that initiation was inhibited by direct damage to ori P. These observations suggested that C-1027 acted in trans to inhibit EBV DNA replication, possibly by induction of a cell cycle checkpoint response. The effect of high levels of DNA damage on mitochondrial replication was limited, indicating that inhibition of mitochondrial replication probably occurred in cis. Thus, nuclear and non-nuclear (mitochondrial) replication differ in their DNA damage response.

Future studies will examine which replication factors are affected by C-1027. Raji cells will be treated with C-1027 and cell extracts assayed for inhibitory potency in an in vitro replication assay. Such studies should elucidate avenues common to agents inducing trans regulation of DNA replication.

ACKNOWLEDGMENT

We are very grateful to Dr. William C. Burhans (Roswell Park Cancer Institute) for useful discussions during the preparation of this manuscript and to Dr. Toshio Otani (Taiho Pharmaceutical Co., Ltd. Haino Research Center, Saitama, 357 Japan) for providing C-1027 and maintaining an interest in our research involving this agent.

REFERENCES

1. Liu, V. F., Boubnov, N. V., and Weaver, D. T. (1995) *Stem Cells 13*, 117−128.
2. Orren, D. K., Petersen, L. N., and Bohr, V. A. (1995) *Mol. Cell. Biol. 15*, 3722−3730.
3. Rhys, C. M., and Bohr, V. A. (1996) *EXS 77*, 289−305.
4. Permana, P. A., and Snapka, R. M. (1994) *Carcinogenesis 15*, 1031−1036.
5. Comess, K. M., Burstyn, J. N., Essigmann, J. M., and Lippard, S. J. (1992) *Biochemistry 31*, 3975−3990.
6. Mirzayans, R., Enns, L., and Paterson, M. C. (1997) *Radiat. Res. 147*, 13−21.
7. Kalejta, R. F., and Hamlin, J. L. (1997) *Exp. Cell Res. 231*, 173−183.
8. Wang, Y., Huq, M. S., Cheng, X., and Iliakis, G. (1995) *Radiat. Res. 142*, 169−175.
9. Wang, Y., Huq, M. S., and Iliakis, G. (1996) *Radiat. Res. 145*, 408−418.
10. Iliakis, G. (1997) *Semin. Oncol. 24*, 602−615.

11. Larner, J. M., Lee, H., and Hamlin, J. L. (1997) *Cancer Surv. 29*, 25−45.
12. Longo, J. A., Nevaldine, B., Longo, S. L., Winfield, J. A., and Hahn, P. J. (1997) *Radiat. Res. 147*, 35−40.
13. McHugh, M. M., Woynarowski, J. M., Gawron, L. S., Otani, T., and Beerman, T. A. (1995) *Biochemistry 34*, 1805−1814.
14. Povirk, L. F., and Goldberg, I. H. (1982) *Biochemistry 21*, 5857−5862.
15. Painter, R. B. (1986) *Int. J. Radiat. Biol. Relat. Stud. Phys., Chem. Med. 49*, 771−781.
16. Gibbons, G. R., Kaufmann, W. K., and Chaney, S. G. (1991) *Carcinogenesis 12*, 2253−2257.
17. Huberman, J. A. (1994) in *The Cell Cycle: A Practical Approach* (Fantes, P., and Brooks, R. F., Eds.) pp 213−234, Oxford University Press, Oxford, U.K.
18. Gilbert, D. M., Neilson, A., Miyazawa, H., DePamphilis, M. L., and Burhans, W. C. (1995) *J. Biol. Chem. 270*, 9597−9606.
19. Cobuzzi, R. J., Burhans, W. C., and Beerman, T. A. (1996) *J. Biol. Chem. 271*, 19852−19859.
20. McHugh, M. M., Beerman, T. A., and Burhans, W. C. (1997) *Biochemistry 36*, 1003−1009.
21. Tooze, S. (1980) *Molecular Biology of Tumor Viruses, pt. 2*, 2nd ed., Cold Springs Harbor Laboratory, Inc., Cold Springs Harbor, NY.
22. Adams, A., and Lindahl, T. (1975) *Proc. Natl. Acad. Sci. U.S.A. 72*, 1477−1481.
23. Hatfull, G., Bankier, A. T., Barrell, B. G., and Farrell, P. J. (1988) *Virology 164*, 334−340.
24. Johnson, P. G., and Beerman, T. A. (1994) *Anal. Biochem. 220*, 103−114.
25. Yang, Q., Hergenhahn, M., and Bartsch, H. (1997) *Carcinogenesis 18*, 1401−1405.
26. Little, R. D., and Schildkraut, C. L. (1995) *Mol. Cell. Biol. 15*, 2893−2903.
27. Gussander, E., and Adams, A. (1984) *J. Virol 52*, 549−556.
28. Hsieh, D. J., Camiolo, S. M., and Yates, J. L. (1993) *EMBO J. 12*, 4933−4944.
29. Jankelevich, S., Kolman, J. L., Bodnar, J. W., and Miller, G. (1992) *EMBO J. 11*, 1165−1176.
30. Yoshida, K.-I., Minami, Y., Azuma, R., Saeki, M., and Otani, T. (1993) *Tetrahedron Lett. 34*, 2637−2640.
31. Hu, J. L., Xue, Y. C., Xie, M. Y., Zhang, R., Otani, T., Minami, Y., Yamada, Y., and Marunaka, T. (1988) *J. Antibiot. 41*, 1575−1579.
32. Yates, J., Warren, N., Reisman, D., and Sugden, B. (1984) *Proc. Natl. Acad. Sci. U.S.A. 81*, 3806−3810.
33. Anderson, S., Bankier, A. T., Barrell, B. G., de Bruijn, M. H., Coulson, A. R., Drouin, J., Eperon, I. C., Nierlich, D. P., Roe, B. A., Sanger, F., Schreier, P. H., Smith, A. J., Staden, R., and Young, I. G. (1981) *Nature 290*, 457−465.
34. Cobuzzi, R. J., Jr., Kotsopoulos, S. K., Otani, T., and Beerman, T. A. (1995) *Biochemistry 34*, 583−592.
35. McHugh, M. M., and Beerman, T. A. (1999) *BioTechniques 26*, 188−190, 192, 194.
36. Reisman, D., Yates, J., and Sugden, B. (1985) *Mol. Cell. Biol. 5*, 1822−1832.
37. Brown, E. H., Iqbal, M. A., Stuart, S., Hatton, K. S., Valinsky, J., and Schildkraut, C. L. (1987) *Mol. Cell. Biol. 7*, 450−457.
38. Beverley, S. M. (1988) *Nucleic Acids Res. 16*, 925−939.
39. Kripalani-Joshi, S., and Law, H. Y. (1994) *Int. J. Cancer 56*, 187−192.
40. Lamb, J. R., Petit-Frere, C., Broughton, B. C., Lehmann, A. R., and Green, M. H. (1989) *Int. J. Radiat. Biol. 56*, 125−130.
41. Crews, S., Ojala, D., Posakony, J., Nishiguchi, J., and Attardi, G. (1979) *Nature 277*, 192−198.
42. Brewer, B. J., and Fangman, W. L. (1988) *Cell 55*, 637−643.
43. Mayhook, A. G., Rinaldi, A. M., and Jacobs, H. T. (1992) *Proc. R. Soc. London, Ser. B: Biol. Sci. 248*, 85−94.
44. Huberman, J. A. (1997) *Methods 13*, 247−257.
45. Friedman, K. L., and Brewer, B. J. (1995) *Methods Enzymol. 262*, 613−627.
46. Larner, J. M., Lee, H., and Hamlin, J. L. (1994) *Mol. Cell. Biol. 14*, 1901−1908.
47. Little, R. D., Platt, T. H., and Schildkraut, C. L. (1993) *Mol. Cell. Biol. 13*, 6600−6613.
48. Xu, Y. J., Li, D. D., and Zhen, Y. S. (1990) *Cancer Chemother. Pharmacol. 27*, 41−46.
49. Brenot-Bosc, F., Gupta, S., Margolis, R. L., and Fotedar, R. (1995) *Chromosoma 103*, 517−527.
50. Kaufmann, W. K., and Kies, P. E. (1998) *Mutat. Res. 400*, 153−167.
51. Cleaver, J. E. (1992) *Radiat. Res. 131*, 338−344.
52. Li, J. J. (1995) *Curr. Biol. 5*, 472−475.
53. Bogenhagen, D., and Clayton, D. A. (1977) *Cell 11*, 719−727.
54. Mancini, M., Anderson, B. O., Caldwell, E., Sedghinasab, M., Paty, P. B., and Hockenbery, D. M. (1997) *J. Cell. Biol. 138*, 449−469.
55. Colacino, J. M., Malcolm, S. K., and Jaskunas, S. R. (1994) *Antimicrob. Agents Chemother. 38*, 1997−2002.
56. Tepper, C. G., and Studzinski, G. P. (1993) *J. Cell. Biochem. 52*, 352−361.
57. Reipert, S., Berry, J., Hughes, M. F., Hickman, J. A., and Allen, T. D. (1995) *Exp. Cell Res. 221*, 281−288.
58. Mignotte, B., and Vayssiere, J. L. (1998) *Eur. J. Biochem. 252*, 1−15.

BI9903143